International Journal of Mechanical, Industrial and Aerospace Sciences
ISSN: 2517-9950
Vol:13, No:9, 2019

Analytical Solution of the Boundary Value Problem of Delaminated Doubly-Curved Composite Shells

András Szekrényes

***Abstract*—**Delamination is one of the major failure modes in laminated composite structures. Delamination tips are mostly captured by spatial numerical models in order to predict crack growth. This paper presents some mechanical models of delaminated composite shells based on shallow shell theories. The mechanical fields are based on a third-order displacement field in terms of the through-thickness coordinate of the laminated shell. The undelaminated and delaminated parts are captured by separate models and the continuity and boundary conditions are also formulated in a general way providing a large size boundary value problem. The system of differential equations is solved by the state space method for an elliptic delaminated shell having simply supported edges. The comparison of the proposed and a numerical model indicates that the primary indicator of the model is the deflection, the secondary is the widthwise distribution of the energy release rate. The model is promising and suitable to determine accurately the J-integral distribution along the delamination front. Based on the proposed model it is also possible to develop finite elements which are able to replace the computationally expensive spatial models of delaminated structures.

***Keywords*—**J-integral, Lévy method, third-order shell theory, state space solution.

I. Introduction

LAMINATED composite materials provide excellent stiffness and strength under mechanical, thermal and chemical environments [1], [2]. The strength properties of laminated composite materials are tailorable in accordance with the loading conditions. This makes these materials versatile and superior over metals and other plastics in many applications. However, from the standpoint of failure laminated composites are more susceptible to the different type of damage modes than metals or isotropic plastics. Such failure modes are fiber breakage, matrix cracking, fiber pull-out, and among others interlaminar facture or delamination [3]. The phenomenon of delamination has been investigated for a long time in the literature. There are many models and approximations available and mainly originated to linear elastic fracture mechanics (LEFM) [4]. The delamination in composite materials is treated as a crack. The appearance of cracks in the material involves significant perturbations in the mechanical fields. Mechanics is indispensable to capture appropriately the effect of cracks and to determine the energy release rate, a quantity characterizing the fracture mechanical behavior of the material. The cracks and delaminations can be classified in accordance with shape, size and extension:

A. Szekrényes is with the Department of Applied Mechanics, Budapest University of Technology and Economics, Budapest, Műegyetem rkp. 5, Building MM, 1111, Hungary (e-mail: szeki@mm.bme.hu).

- 1D cracks are mainly captured by beam specimens and advanced beam models to get acquainted with the influence of material defects on the fracture behavior. Many beam models have been developed in mechanics involving the equivalent single layer (ESL) and layerwise formulations [5]-[9]. The most important aspect of the mathematical models is that the governing equations contain single variable functions of displacement variables.
- 2D flat cracks occur mainly in plate like structures meaning that the material defect extends in two independent directions in the plane of crack [10]-[13]. This problem is significantly more complicated than the modelling of 1D cracks, because the governing equations are partial differential equations (PDE).
- 3D cracks and delaminations can take place in laminated structures with general shape. Some particular cases in the field of composite structures are: cylindrical and conical shells and - involving the former two ones as special cases - composite doubly-curved shells [14]. Shells are more complex structures than flat plates, since the mathematical formulation requires more variables and parameters [15], [16]. As a matter of fact, doubly curved shells have two independent radii of curvature, the formulation should be done in curvilinear coordinate system, and finally but not least, the governing equations are more complicated and lengthy than those of plates.

Independently of the type of continuum models (beam, plate or shell) the model formulation can be classified by:

- ESL theories, in which the heterogeneous laminated structure is treated as a statically ESL having complex constitutive behavior [2], [17].
- Partial layerwise theories capturing the whole laminate as sublaminates taking transverse shear deformation into consideration, in other words the in-plane or in-surface displacements are described by higher-order functions. However the normal strain is not accounted for [2], [18], [19].
- Full layerwise models are based on the layerwise expansion of the three dimensional displacement field leading to transversely and normally deformable models. This formulation is also called as zig-zag model [2], [20], [21].

Layerwise models provide kinematically more correct solution than ESL models. However, the computational cost is significantly higher as well. Thus, layerwise models should be applied only if these are required. Such a case is the delaminated plates and shells, in which the perturbation of

mechanical fields is significant and higher-order layerwise theories are required to have accurate results.

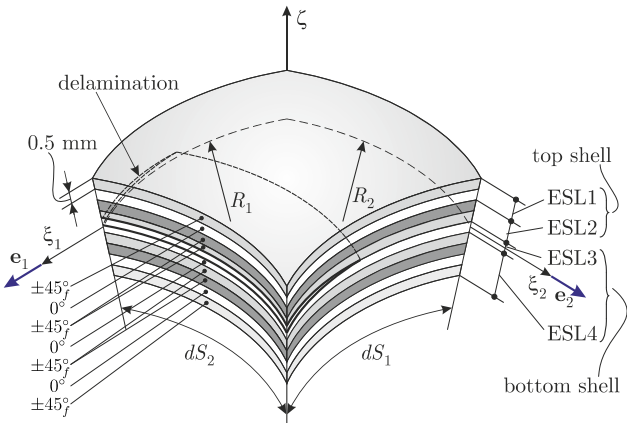

Fig. 1 Shell element with orthotropic plies and the position of delamination over the shell thickness

The main aspect of this paper compared to the existing works is that the effect of delamination is captured by the locally accurate mechanical fields and the 3D J-integral [22], [23] is determined along the delamination front. Moreover, the proposed model is a nonsingular continuum model without the usual singularity assumed by fracture mechanics. This paper is arranged in accordance with the following. In Section II the layerwise displacement field is presented together with the continuity conditions along the thicknesswise direction. Section III presents strain and stress field equations of laminated shells. In Section IV the governing equations are derived by the principle of virtual work. The system of PDEs is solved in Section V and Sections VI-VIII present the results.

II. Partial Semi-Layerwise Displacement Field and Continuity Conditions

The proposed modelling technique belongs to the partial semi-layerwise theories, i.e., the thicknesswise elasticity of the laminate is left out of consideration. Fig. 1 shows a differential shell element with delamination. The whole laminate is captured by four ESLs; two ESLs are applied below and above the delamination (shaded area). The equations of undelaminated and delaminated regions are presented separately.

A. Undelaminated Part

The general third-order Taylor-expansion of the in-surface displacement functions result in the following displacement field:

$$u_{(i)}(\xi_1,\xi_2,\zeta^{(i)}) = u_0(\xi_1,\xi_2) + u_{0i}(\xi_1,\xi_2) + \theta_{(\xi_1)i}(\xi_1,\xi_2)\zeta^{(i)} + \phi_{(\xi_1)i}(\xi_1,\xi_2)[\zeta^{(i)}]^2 + \lambda_{(\xi_1)i}(\xi_1,\xi_2)[\zeta^{(i)}]^3,$$

$$v_{(i)}(\xi_1,\xi_2,\zeta^{(i)}) = v_0(\xi_1,\xi_2) + v_{0i}(\xi_1,\xi_2) + \theta_{(\xi_2)i}(\xi_1,\xi_2)\zeta^{(i)} + \phi_{(\xi_2)i}(\xi_1,\xi_2)[\zeta^{(i)}]^2 + \lambda_{(\xi_2)i}(\xi_1,\xi_2)[\zeta^{(i)}]^3,$$

$$w_{(i)}(\xi_1,\xi_2) = w(\xi_2,\xi_2), \quad (1)$$

where i = 1..4 is the index of the actual ESL, $\zeta^{(i)}$ is the local through thickness coordinate of the i^{th} ESL and always coincides with the local midplane, u_0 and v_0 are the global, u_{0i} and v_{0i} are the local membrane displacements, moreover, θ means the rotations of cross sections about the ξ_1 and ξ_2 axes, ϕ denotes the second-order, λ represents the third-order terms in the displacement functions. Finally $w_{(i)}$ is the transverse deflection function. Equation (1), which is the idea of third-order shear deformable shell theory (TST), will be applied equally to the undelaminated and delaminated portions and the continuity between these parts will be established. In this work only shear deformable shell models are developed, in other words the deflection is inextensible in the through-thickness direction involving that $w_{(i)}(\xi_1, \xi_2) = w(\xi_1, \xi_2)$. The displacement functions of first-order (FST) and second- order shear deformable shell theory (SST) can be obtained by reducing (1) and taking $\phi_{(\xi1)i} = \phi_{(\xi2)i} = 0$ and $\lambda_{(\xi1)i} = \lambda_{(\xi2)i} = 0$, respectively [24], [25]. The displacement field given by (1) is associated to each ESL.

The displacement vector field for the i^{th} ESL is $\mathbf{u}_{(i)} = (u_{(i)}\ v_{(i)}\ w_{(i)})^T$. The layerwise kinematic continuity between the displacement fields of adjacent ESLs is established by the system of exact kinematic conditions (SEKC), which was originally developed in [13], [18], [19], [26], [27]. The first set of conditions formulates the continuity of the in-surface (ξ_1, ξ_2) and transverse (ζ) displacements between the neighboring plies as:

$$(u_{(1)}, v_{(1)}, w_{(1)})|_{\zeta^{(1)}=t_1/2} = (u_{(2)}, v_{(2)}, w_{(2)})|_{\zeta^{(2)}=-t_2/2},$$

$$(u_{(2)}, v_{(2)}, w_{(2)})|_{\zeta^{(2)}=t_2/2} = (u_{(3)}, v_{(3)}, w_{(3)})|_{\zeta^{(3)}=-t_3/2},$$

$$(u_{(3)}, v_{(3)}, w_{(3)})|_{\zeta^{(3)}=t_3/2} = (u_{(4)}, v_{(4)}, w_{(4)})|_{\zeta^{(4)}=-t_4/2}. \quad (2)$$

where t_i, i = 1..4 are the thicknesses of ESLs. The second set of conditions defines the global membrane displacements (u_0, v_0) at the reference surface of the actual region. The reference surface belongs to the second ESL (see Fig. 1); therefore, the following condition is imposed:

$$(u_{(2)}, v_{(2)})|_{\zeta^{(2)}=\zeta_R^{(2)}} = (u_0(\xi_1,\xi_2), v_0(\xi_1,\xi_2)), \quad (3)$$

where $\zeta_R^{(2)} = 1/2(t_3 + t_4 - t_1)$ is the position of the global midsurface of the model with respect to ESL2. The next set of conditions imposes the continuous shear strains at the interface surfaces [11]:

$$(\gamma_{1\zeta(1)}, \gamma_{2\zeta(1)})|_{\zeta^{(1)}=t_1/2} = (\gamma_{1\zeta(2)}, \gamma_{2\zeta(2)})|_{\zeta^{(2)}=-t_2/2},$$

$$(\gamma_{1\zeta(2)}, \gamma_{2\zeta(2)})|_{\zeta^{(2)}=t_2/2} = (\gamma_{1\zeta(3)}, \gamma_{2\zeta(3)})|_{\zeta^{(3)}=-t_3/2},$$

$$(\gamma_{1\zeta(3)}, \gamma_{2\zeta(3)})|_{\zeta^{(3)}=t_3/2} = (\gamma_{1\zeta(4)}, \gamma_{2\zeta(4)})|_{\zeta^{(4)}=-t_4/2}. \quad (4)$$

The oscillations in the shear strain distribution can be reduced by ensuring continuous shear strain derivatives at interface surfaces 1-2 and 3-4:

TABLE I
PRIMARY PARAMETERS OF THE DIFFERENT SHELL THEORIES, UNDELAMINATED PART, $P = \xi_1$ OR ξ_2

TST	$\theta_{(p)1}$, $\theta_{(p)2}$, $\theta_{(p)3}$, $\theta_{(p)4}$, $\lambda_{(p)3}$
SST	$\theta_{(p)2}$, $\boxed{\phi_{(p)2}}$, $\theta_{(p)4}$, $\phi_{(p)4}$
FST	$\theta_{(p)1}$, $\theta_{(p)2}$, $\theta_{(p)3}$, $\theta_{(p)4}$

TABLE II
PRIMARY PARAMETERS OF THE DIFFERENT SHELL THEORIES, DELAMINATED PART, $P = \xi_1$ OR ξ_2

TST	$\theta_{(p)1}$, $\theta_{(p)2}$, $\theta_{(p)3}$, $\theta_{(p)4}$, $\boxed{\lambda_{(p)1}}$, $\lambda_{(p)3}$
SST	$\theta_{(p)2}$, $\theta_{(p)4}$, $\phi_{(p)4}$
FST	$\theta_{(p)1}$, $\theta_{(p)2}$, $\theta_{(p)3}$, $\theta_{(p)4}$

$$(\frac{\partial\gamma_{1\zeta(1)}}{\partial\zeta^{(1)}},\frac{\partial\gamma_{2\zeta(1)}}{\partial\zeta^{(1)}})|_{\zeta^{(1)}=t_1/2} = (\frac{\partial\gamma_{1\zeta(2)}}{\partial\zeta^{(2)}},\frac{\partial\gamma_{2\zeta(2)}}{\partial\zeta^{(2)}})|_{\zeta^{(2)}=-t_2/2},$$

$$(\frac{\partial\gamma_{1\zeta(3)}}{\partial\zeta^{(3)}},\frac{\partial\gamma_{2\zeta(3)}}{\partial\zeta^{(3)}})|_{\zeta^{(3)}=t_3/2} = (\frac{\partial\gamma_{1\zeta(4)}}{\partial\zeta^{(4)}},\frac{\partial\gamma_{2\zeta(4)}}{\partial\zeta^{(4)}})|_{\zeta^{(4)}=-t_4/2}, \quad (5)$$

The continuity of the second derivatives of shear strains with respect to the through-thickness coordinate at the interface planes involves the following conditions:

$$(\frac{\partial^2\gamma_{1\zeta(1)}}{\partial(\zeta^{(1)})^2},\frac{\partial^2\gamma_{2\zeta(1)}}{\partial(\zeta^{(1)})^2})|_{\zeta^{(1)}=\frac{t_1}{2}} = (\frac{\partial^2\gamma_{1\zeta(2)}}{\partial(\zeta^{(2)})^2},\frac{\partial^2\gamma_{2\zeta(2)}}{\partial(\zeta^{(2)})^2})|_{\zeta^{(2)}=-\frac{t_2}{2}},$$

$$(\frac{\partial^2\gamma_{1\zeta(3)}}{\partial(\zeta^{(3)})^2},\frac{\partial^2\gamma_{2\zeta(3)}}{\partial(\zeta^{(3)})^2})|_{\zeta^{(3)}=\frac{t_3}{2}} = (\frac{\partial^2\gamma_{1\zeta(4)}}{\partial(\zeta^{(4)})^2},\frac{\partial^2\gamma_{2\zeta(4)}}{\partial(\zeta^{(4)})^2})|_{\zeta^{(4)}=-\frac{t_4}{2}}. \quad (6)$$

To further reduce the number of parameters, the so-called shear strain control condition (SSCC, [11]) is applied at the top and bottom boundaries of the undelaminated part:

$$(\gamma_{1\zeta(1)},\gamma_{2\zeta(1)})|_{\zeta^{(1)}=-t_1/2} = (\gamma_{1\zeta(4)},\gamma_{2\zeta(4)})|_{\zeta^{(4)}=t_4/2}. \quad (7)$$

In (1) the displacement functions are modified in order to satisfy (2)-(15). In the general sense, by applying the FST, SST and TST theories the in-surface displacement functions can be written as:

$$u_{(i)}(\xi_1,\xi_2,\zeta) = u_0(\xi_1,\xi_2) + (K_{ij}^{(0)} + K_{ij}^{(1)}\zeta^{(i)} + K_{ij}^{(2)}[\zeta^{(i)}]^2 + K_{ij}^{(3)}[\zeta^{(i)}]^3)\psi_{(1)j}, \quad (8)$$

$$v_{(i)}(\xi_1,\xi_2,\zeta) = v_0(\xi_1,\xi_2) + (K_{ij}^{(0)} + K_{ij}^{(1)}\zeta^{(i)} + K_{ij}^{(2)}[\zeta^{(i)}]^2 + K_{ij}^{(3)}[\zeta^{(i)}]^3)\psi_{(1)j}, \quad (9)$$

$$w_{(i)}(\xi_1,\xi_2,\zeta) = w(\xi_1,\xi_2), \quad (10)$$

where K_{ij} is the displacement multiplicator matrix and related exclusively to the geometry (ESL thicknesses), i refers to the ESL number, the summation index j defines the component in $\boldsymbol{\psi}$, which is the vector of primary parameters, finally $w_{(i)}(\xi_1, \xi_2) = w(\xi_1, \xi_2)$ for each ESLs, i.e. the transverse normal of each ESL is inextensible [2]. Equations (8) and (9) can be obtained by parameter elimination [28]. It is important to note that the size and the elements of $\boldsymbol{\psi}$ depend on the applied theory, the number of ESLs and the number of conditions applied. Tables I and II collect a possible choice of primary parameters for the undelaminated and delaminated parts as well. The parameters in rectangle are the so-called autocontinuity parameters [19]. The corresponding K_{ij} multiplicator matrix elements are given in [28] for each theory.

B. Delaminated Part

In the delaminated region (refer to Fig. 1) the top and bottom surfaces are equally modeled by two ESLs, and thus the first and third of (2) still hold in each theory. In accordance with (2) the transverse deflections of the top and bottom shells of the delaminated region are identical (constrained mode model, [13]). The definition of the top and bottom reference surfaces involves:

$$(u_{(1)},v_{(1)})|_{\zeta^{(1)}=t_2/2} = (u_{0b}(\xi_1,\xi_2),v_{0b}(\xi_1,\xi_2)),$$
$$(u_{(3)},v_{(3)})|_{\zeta^{(3)}=t_4/2} = (u_{0t}(\xi_1,\xi_2),v_{0t}(\xi_1,\xi_2)), \quad (11)$$

where u_{0b}, v_{0b} and u_{0t}, v_{0t} are the global membrane displacements of the bottom and top shells. Furthermore, the first and third conditions by (4) apply again, as well as (5) and (6). Three more equations are formulated by using SSCC:

$$(\gamma_{1\zeta(1)},\gamma_{2\zeta(1)})|_{\zeta^{(1)}=-t_1/2} = (\gamma_{1\zeta(2)},\gamma_{2\zeta(2)})|_{\zeta^{(2)}=t_2/2},$$
$$(\gamma_{1\zeta(3)},\gamma_{2\zeta(3)})|_{\zeta^{(3)}=-t_3/2} = (\gamma_{1\zeta(4)},\gamma_{2\zeta(4)})|_{\zeta^{(4)}=t_4/2},$$
$$(\gamma_{1\zeta(1)},\gamma_{2\zeta(1)})|_{\zeta^{(1)}=-t_1/2} = (\gamma_{1\zeta(4)},\gamma_{2\zeta(4)})|_{\zeta^{(4)}=t_4/2}, \quad (12)$$

Using the equations above the displacement field is given by:

$$u_{(i)}(\xi_1,\xi_2,\zeta) = u_{0b}(\xi_1,\xi_2) + (K_{ij}^{(0)} + K_{ij}^{(1)}\zeta^{(i)} + K_{ij}^{(2)}[\zeta^{(i)}]^2 + K_{ij}^{(3)}[\zeta^{(i)}]^3)\psi_{(1)j}, i = 1..2,$$
$$v_{(i)}(\xi_1,\xi_2,\zeta) = v_{0b}(\xi_1,\xi_2) + (K_{ij}^{(0)} + K_{ij}^{(1)}\zeta^{(i)} + K_{ij}^{(2)}[\zeta^{(i)}]^2 + K_{ij}^{(3)}[\zeta^{(i)}]^3)\psi_{(2)j}, i = 1..2, \quad (13)$$

$$u_{(i)}(\xi_1,\xi_2,\zeta) = u_{0t}(\xi_1,\xi_2) + (K_{ij}^{(0)} + K_{ij}^{(1)}\zeta^{(i)} + K_{ij}^{(2)}[\zeta^{(i)}]^2 + K_{ij}^{(3)}[\zeta^{(i)}]^3)\psi_{(1)j}, i = 3..4,$$
$$v_{(i)}(\xi_1,\xi_2,\zeta) = v_{0t}(\xi_1,\xi_2) + (K_{ij}^{(0)} + K_{ij}^{(1)}\zeta^{(i)} + K_{ij}^{(2)}[\zeta^{(i)}]^2 + K_{ij}^{(3)}[\zeta^{(i)}]^3)\psi_{(2)j}, i = 3..4,$$
$$w_{(i)}(\xi_1,\xi_2,\zeta) = w(\xi_1,\xi_2), i = 1..4, \quad (14)$$

where the K_{ij} multiplicator matrix elements can be obtained by applying the above mentioned equations to (1). The K_{ij} elements are given in [28].

III. STRAIN AND STRESS FIELDS

The strain-displacement relation of doubly-curved shells can be written as [2]:

$$\varepsilon_{1(i)} = \frac{1}{A_1}(\frac{\partial u_{(i)}}{\partial\xi_1} + \frac{1}{a_2}\frac{\partial a_1}{\partial\xi_2}v_{(i)} + \frac{a_1}{R_1}w),$$
$$\varepsilon_{2(i)} = \frac{1}{A_2}(\frac{\partial v_{(i)}}{\partial\xi_2} + \frac{1}{a_1}\frac{\partial a_2}{\partial\xi_1}u_{(i)} + \frac{a_2}{R_2}w),$$
$$\gamma_{12(i)} = \frac{A_2}{A_1}\frac{\partial}{\partial\xi_1}(\frac{v_{(i)}}{A_2}) + \frac{A_1}{A_2}\frac{\partial}{\partial\xi_2}(\frac{u_{(i)}}{A_2}), \quad (15)$$

$$\gamma_{23(i)} = \frac{1}{A_2}\frac{\partial w}{\partial \xi_2} + A_2 \frac{\partial}{\partial \zeta^{(i)}}\left(\frac{v_{(i)}}{A_2}\right),$$
$$\gamma_{13(i)} = \frac{1}{A_1}\frac{\partial w}{\partial \xi_1} + A_1 \frac{\partial}{\partial \zeta^{(i)}}\left(\frac{u_{(i)}}{A_1}\right), \quad (16)$$

where $A_1 = a_1(1+\zeta^{(i)}/R_1), A_2 = a_2(1+\zeta^{(i)}/R_2)$ are the Lamé parameters, a_1 and a_2 are the scale factors, R_1 and R_2 are the radii of curvatures in both directions.

Applying (15)-(16) to the displacement field by (8)-(10) for the undelaminated part yields:

$$\begin{pmatrix}\varepsilon_1\\ \varepsilon_2\\ \gamma_{12}\end{pmatrix}_{(i)} = \begin{pmatrix}\varepsilon_1^{(0)}\\ \varepsilon_2^{(0)}\\ \gamma_{12}^{(0)}\end{pmatrix} + \zeta^{(i)}\begin{pmatrix}\varepsilon_1^{(1)}\\ \varepsilon_2^{(1)}\\ \gamma_{12}^{(1)}\end{pmatrix} + [\zeta^{(i)}]^2\begin{pmatrix}\varepsilon_1^{(2)}\\ \varepsilon_2^{(2)}\\ \gamma_{12}^{(2)}\end{pmatrix} + [\zeta^{(i)}]^3\begin{pmatrix}\varepsilon_1^{(3)}\\ \varepsilon_2^{(3)}\\ \gamma_{12}^{(3)}\end{pmatrix}. \quad (17)$$

The vector of transverse shear strains is:

$$\begin{pmatrix}\gamma_{1\zeta}\\ \gamma_{2\zeta}\end{pmatrix}_{(i)} = \begin{pmatrix}\gamma_{1\zeta}^{(0)}\\ \gamma_{2\zeta}^{(0)}\end{pmatrix}_{(i)} + \zeta^{(i)}\cdot\begin{pmatrix}\gamma_{1\zeta}^{(1)}\\ \gamma_{2\zeta}^{(1)}\end{pmatrix}_{(i)} + [\zeta^{(i)}]^2\cdot\begin{pmatrix}\gamma_{1\zeta}^{(2)}\\ \gamma_{2\zeta}^{(2)}\end{pmatrix}_{(i)}. \quad (18)$$

To determine the stress field, we apply the constitutive equation for orthotropic materials under plane stress state, which is $\boldsymbol{\sigma}^{(m)}{}_{(i)} = \overline{\boldsymbol{C}}^{(m)}{}_{(i)}\boldsymbol{\varepsilon}^{(m)}$ [2], [17], leading to:

$$\begin{pmatrix}\sigma_1\\ \sigma_2\\ \tau_{2\zeta}\\ \tau_{1\zeta}\\ \tau_{12}\end{pmatrix}_{(i)}^{(m)} = \begin{pmatrix}\overline{C}_{11} & \overline{C}_{12} & 0 & 0 & 0\\ \overline{C}_{12} & \overline{C}_{22} & 0 & 0 & 0\\ 0 & 0 & \overline{C}_{44} & 0 & 0\\ 0 & 0 & 0 & \overline{C}_{55} & 0\\ 0 & 0 & 0 & 0 & \overline{C}_{66}\end{pmatrix}_{(i)}^{(m)}\begin{pmatrix}\varepsilon_1\\ \varepsilon_2\\ \gamma_{2\zeta}\\ \gamma_{1\zeta}\\ \gamma_{12}\end{pmatrix}_{(i)}, \quad (19)$$

where $\boldsymbol{C}^{(m)}{}_{(i)}$ is the stiffness matrix of the m^{th} layer within the i^{th} ESL. For the delaminated part, the form of the strain and stress fields are the same as those by (17), (18), however (13), (14) have to be involved when (15) and (16) are applied.

IV. The Governing PDE

To derive the governing equations of the shell system we apply the virtual work principle [2]:

$$\int_{T_0}^{T_1}(\delta\mathcal{U} - \delta\mathcal{W}_F)\,dt = 0, \delta\mathcal{U} = \sum_i \delta\mathcal{U}_{(i)}, \delta\mathcal{W}_F = \sum_i \delta\mathcal{W}_{F(i)} \quad (20)$$

where U is the strain energy, W_F is the work of external forces and t is the time ($L = U - W_F$ is the Lagrange function). To derive the equilibrium equations of the shell system in a compact and invariant form, we define the following vectors:

$$\mathbf{N}_i^{(1,12)} = (N_1 \quad N_{12})_{(i)}^T, \mathbf{N}_i^{(12,3)} = (N_{12} \quad N_2)_{(i)}^T,$$
$$\mathbf{M}_i^{(1,12)} = (M_1 \quad M_{12})_{(i)}^T, \mathbf{M}_i^{(12,2)} = (M_{12} \quad M_2)_{(i)}^T, \quad (21)$$

The vectors of higher-order stress resultants become:

$$\mathbf{L}_i^{(1,12)} = (L_1 \quad L_{12})_{(i)}^T, \mathbf{L}_i^{(12,2)} = (L_{12} \quad L_2)_{(i)}^T,$$
$$\mathbf{P}_i^{(1,12)} = (P_1 \quad P_1)_{(i)}^T, \mathbf{P}_i^{(12,2)} = (P_{12} \quad P_2)_{(i)}^T. \quad (22)$$

Finally, the vector of shear forces becomes:

$$\mathbf{Q}_i = (Q_1 \quad Q_2)_{(i)}^T \quad (23)$$

In the sequel, the equilibrium equations are derived separatelyfor the undelaminated and delaminated regions.

A. Undelaminated Part

The application of virtual work principle [2] to the undelaminated region of the shell leads to three sets of equations. The first set is related to the in-surface equilibrium of the following stress resultants:

$$\delta u_0: \sum_{i=1}^{4} \hat{\boldsymbol{\nabla}}\cdot\mathbf{N}^{(1,12)} + \frac{a_1a_2}{R_1}Q_{1(i)} + \frac{a_1}{2}\left(\frac{1}{R_1} - \frac{1}{R_2}\right)M_{12(i),2} = 0,$$
$$\delta v_0: \sum_{i=1}^{4} \hat{\boldsymbol{\nabla}}\cdot\mathbf{N}^{(12,2)} + \frac{a_1a_2}{R_2}Q_{2(i)} - \frac{a_1}{2}\left(\frac{1}{R_1} - \frac{1}{R_2}\right)M_{12(i),1} = 0, \quad (24)$$

where $\hat{\boldsymbol{\nabla}} = a_2(..)_{,1}\mathbf{e}_1 + a_1(..)_{,2}\mathbf{e}_2$. The second set of equations is related to the elements of the vector of primary parameters:

$$\begin{matrix}\delta\psi_{(1)j}:\\ \delta\psi_{(2)j}:\end{matrix}\Bigg\}\sum_{i=1}^{4} K_{ij}^{(0)}\begin{pmatrix}\hat{\boldsymbol{\nabla}}\cdot\mathbf{N}^{(1,12)}\\ \hat{\boldsymbol{\nabla}}\cdot\mathbf{N}^{(12,2)}\end{pmatrix} + K_{ij}^{(1)}\begin{pmatrix}\hat{\boldsymbol{\nabla}}\cdot\mathbf{M}^{(1,12)}\\ \hat{\boldsymbol{\nabla}}\cdot\mathbf{M}^{(12,2)}\end{pmatrix} + K_{ij}^{(2)}\begin{pmatrix}\hat{\boldsymbol{\nabla}}\cdot\mathbf{L}^{(1,12)}\\ \hat{\boldsymbol{\nabla}}\cdot\mathbf{L}^{(12,2)}\end{pmatrix} + K_{ij}^{(3)}\begin{pmatrix}\hat{\boldsymbol{\nabla}}\cdot\mathbf{P}^{(1,12)}\\ \hat{\boldsymbol{\nabla}}\cdot\mathbf{P}^{(12,2)}\end{pmatrix} - a_1a_2\begin{pmatrix}(R_1K_{ij}^{(1)} - K_{ij}^{(0)})/R_1\cdot Q_{1(i)}\\ (R_2K_{ij}^{(1)} - K_{ij}^{(0)})/R_2\cdot Q_{2(i)}\end{pmatrix} - 2a_1a_2K_{ij}^{(2)}\begin{pmatrix}R_{1(i)}\\ R_{2(i)}\end{pmatrix} - a_1a_2\begin{pmatrix}(3R_1K_{ij}^{(3)} + K_{ij}^{(2)})/R_1\cdot S_{1(i)}\\ (3R_2K_{ij}^{(3)} + K_{ij}^{(2)})/R_2\cdot S_{2(i)}\end{pmatrix} = \begin{pmatrix}0\\ 0\end{pmatrix}. \quad (25)$$

The last equation represents the equilibrium of shear and membrane forces:

$$\sum_{i=1}^{4} \hat{\boldsymbol{\nabla}}\cdot\mathbf{Q}_i - a_1a_2\sum_{i=1}^{k}\left(\frac{N_{1(i)}}{R_1} + \frac{N_{2(i)}}{R_2}\right) + q = 0, \quad (26)$$

where q is the function of external load. As a next step we write the equilibrium equations in Cartesian coordinate system (x, y and ζ) by:

$$\frac{\partial}{\partial x} = \frac{1}{a_1}\frac{\partial}{\partial \xi_1}, \frac{\partial}{\partial y} = \frac{1}{a_2}\frac{\partial}{\partial \xi_2}. \quad (27)$$

Applying (27) and dividing (24)-(26) by a_1a_2 it is possible to obtain:

$$\delta u_0: \sum_{i=1}^{4} \nabla\cdot\mathbf{N}^{(1,12)} + \frac{Q_{1(i)}}{R_1} + C_0M_{12(i),y} = 0,$$

$$\delta v_0: \sum_{i=1}^{4} \nabla \cdot \mathbf{N}^{(12,2)} + \frac{Q_{2(i)}}{R_2} - C_0\, M_{12(i),x} = 0, \quad (28)$$

where:

$$C_0 = \frac{a_1}{2}\left(\frac{1}{R_1} - \frac{1}{R_2}\right). \quad (29)$$

Moreover, we have:

$$\begin{matrix}\delta\psi_{(1)j}: \\ \delta\psi_{(2)j}:\end{matrix}\Bigg\} \sum_{i=1}^{4} K_{ij}^{(0)} \begin{pmatrix}\nabla\cdot\mathbf{N}^{(1,12)} \\ \nabla\cdot\mathbf{N}^{(12,2)}\end{pmatrix} + K_{ij}^{(1)} \begin{pmatrix}\nabla\cdot\mathbf{M}^{(1,12)} \\ \nabla\cdot\mathbf{M}^{(12,2)}\end{pmatrix} + K_{ij}^{(2)} \begin{pmatrix}\nabla\cdot\mathbf{L}^{(1,12)} \\ \nabla\cdot\mathbf{L}^{(12,2)}\end{pmatrix} + K_{ij}^{(3)} \begin{pmatrix}\nabla\cdot\mathbf{P}^{(1,12)} \\ \nabla\cdot\mathbf{P}^{(12,2)}\end{pmatrix} - \begin{pmatrix}(R_1K_{ij}^{(1)} - K_{ij}^{(0)})/R_1\cdot Q_{1(i)} \\ (R_2K_{ij}^{(1)} - K_{ij}^{(0)})/R_2\cdot Q_{2(i)}\end{pmatrix} - 2K_{ij}^{(2)} \begin{pmatrix}R_{1(i)} \\ R_{2(i)}\end{pmatrix} - \begin{pmatrix}(3R_1K_{ij}^{(3)} + K_{ij}^{(2)})/R_1\cdot S_{1(i)} \\ (3R_2K_{ij}^{(3)} + K_{ij}^{(2)})/R_2\cdot S_{2(i)}\end{pmatrix} = \begin{pmatrix}0 \\ 0\end{pmatrix}. \quad (30)$$

The equation of shear and in-surface forces reduces to:

$$\sum_{i=1}^{k} \boldsymbol{\nabla} \cdot \mathrm{Q}_i - \sum_{i=1}^{k} \left(\frac{N_{1(i)}}{R_1} + \frac{N_{2(i)}}{R_2}\right) + q = 0. \quad (31)$$

The stress resultants in (28)-(31) are determined based on the assumption of shallow shells by assuming that $1+\zeta/R_1 \cong 1$ and $1+\zeta/R_2 \cong 1$ [2]. Thus, in this case the stress resultants are approximated as:

$$\begin{pmatrix}N_{\alpha\beta} \\ M_{\alpha\beta} \\ L_{\alpha\beta} \\ P_{\alpha\beta}\end{pmatrix}_{(i)} = \int_{-t_i/2}^{t_i/2} \sigma_{\alpha\beta} \begin{pmatrix}1 \\ \zeta \\ \zeta^2 \\ \zeta^3\end{pmatrix}_{(i)} d\zeta^{(i)},$$
$$\begin{pmatrix}Q_\alpha \\ R_\alpha \\ S_\alpha\end{pmatrix}_{(i)} = \int_{-t_i/2}^{t_i/2} \tau_{\alpha\zeta} \begin{pmatrix}1 \\ \zeta \\ \zeta^2\end{pmatrix}_{(i)} d\zeta^{(i)}, \quad (32)$$

where α and β take 1 or 2. Taking the constitutive law by (19) back into (32) yields [2], [28]:

$$\begin{pmatrix}\{N\} \\ \{M\} \\ \{L\} \\ \{P\}\end{pmatrix}_{(i)} = \begin{pmatrix}[A] & [B] & [D] & [E] \\ [B] & [D] & [E] & [F] \\ [D] & [E] & [F] & [G] \\ [E] & [F] & [G] & [H]\end{pmatrix}_{(i)} \begin{pmatrix}\{\varepsilon^{(0)}\} \\ \{\varepsilon^{(1)}\} \\ \{\varepsilon^{(2)}\} \\ \{\varepsilon^{(3)}\}\end{pmatrix}_{(i)}, \quad (33)$$

$$\begin{pmatrix}\{Q\} \\ \{R\} \\ \{S\}\end{pmatrix}_{(i)} = \begin{pmatrix}[A] & [B] & [D] \\ [B] & [D] & [E] \\ [D] & [E] & [F]\end{pmatrix}_{(i)} \begin{pmatrix}\{\gamma^{(0)}\} \\ \{\gamma^{(1)}\} \\ \{\gamma^{(2)}\}\end{pmatrix}_{(i)}, \quad (34)$$

where A_{pq} is the extensional, B_{pq} is coupling, D_{pq} is the bending, E_{pq}, F_{pq}, G_{pq} and H_{pq} are higher-order stiffnesses defined as [28]:

$$(A_{pq}, B_{pq}, D_{pq}, E_{pq}, F_{pq}, G_{pq}, H_{pq})_{(i)} = \sum_{m=1}^{N_{l(i)}} \int_{\zeta_m^{(i)}}^{\zeta_{m+1}^{(i)}} \overline{C}_{pq}^{(m)} (1, \zeta, \zeta^2, \zeta^3, \zeta^4, \zeta^5, \zeta^6)^{(i)} d\zeta^{(i)}, \quad (35)$$

B. Delaminated Part

Utilizing (13), (14) by formulating (20) (similarly to the undelaminated region) results in the equilibrium equations of in-surface forces below:

$$\begin{aligned}\delta u_{0b}: &\sum_{i=1}^{2} \left(\boldsymbol{\nabla} \cdot \mathbf{N}^{(1,12)} + \frac{Q_{1(i)}}{R_1} + C_0 M_{12(i),y}\right) = 0, \\ \delta u_{0t}: &\sum_{i=3}^{4} \left(\boldsymbol{\nabla} \cdot \mathbf{N}^{(1,12)} + \frac{Q_{1(i)}}{R_1} + C_0 M_{12(i),y}\right) = 0, \\ \delta v_{0b}: &\sum_{i=1}^{2} \left(\boldsymbol{\nabla} \cdot \mathbf{N}^{(12,2)} + \frac{Q_{2(i)}}{R_2} - C_0 M_{12(i),x}\right) = 0, \\ \delta v_{0t}: &\sum_{i=3}^{4} \left(\boldsymbol{\nabla} \cdot \mathbf{N}^{(12,2)} + \frac{Q_{2(i)}}{R_2} - C_0 M_{12(i),x}\right) = 0 \end{aligned} \quad (36)$$

The form of the other equilibrium equations is the same as those given by (30) and (31).

V. Lévy Method and State Space Solution

Analytical solution of the presented system of PDEs is possible under Lévy type boundary conditions. Fig. 2 shows a simply supported delaminated shell built-up by layers made out of orthotropic material. The shell is divided into four parts: 1, 1q and 1a are the parts of the delaminated region, 2 is the undelaminated region. For each region the models presented in Sections II-IV should be applied. The basic idea of Lévy formulation is that the primary displacement parameters (presented in Tables I and II), the external load parameter, q in (31), the deflection, $w(x,y)$ and the membrane displacements are expressed by trial functions in the form of:

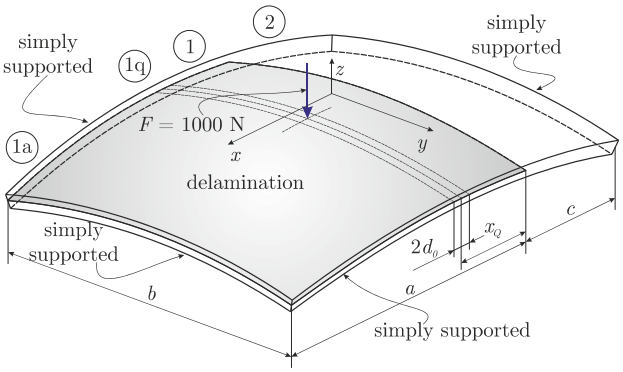

Fig. 2 Simply supported doubly-curved elliptical delaminated composite shell subjected to a concentrated force

$$\begin{pmatrix}\psi_{(1)i}(x,y) \\ \psi_{(2)i}(x,y)\end{pmatrix} = \sum_{n=1}^{\infty} \begin{pmatrix}\Phi_{(1)in}(x)\sin\beta y \\ \Phi_{(2)in}(x)\cos\beta y\end{pmatrix},$$
$$\begin{pmatrix}u(x,y) \\ v(x,y) \\ q(x,y) \\ w(x,y)\end{pmatrix} = \sum_{n=1}^{\infty} \begin{pmatrix}U_n(x)\sin\beta y \\ V_n(x)\cos\beta y \\ Q_n(x)\sin\beta y \\ W_n(x)\sin\beta y\end{pmatrix}, \quad (37)$$

where $\beta = n\pi/b$, b is the shell width (see Fig. 2). By taking back the trial functions in (37) into the strain field (17), (18), then by expressing the stress resultants in accordance with (33), (34) we can utilize the equilibrium equations given by

(28)-(31) and (36) to reduce the system of PDEs to system of ODEs, which can be solved by the state-space approach [29]. The state-space model of the shell system takes the form below [2], [29]:

$$\mathbf{Z}' = \mathbf{TZ} + \mathbf{F}, \tag{38}$$

where **Z** is the state vector, **T** is the system matrix, **F** is the vector of particular solutions, the comma means differentiation with respect to *x*. The general solution of (38) becomes [29]:

$$\mathbf{Z}(x) = e^{\mathbf{T}x}(\mathbf{K} + \int_{x^*}^{x} e^{-\mathbf{T}\xi}\,\mathbf{F}(\xi)d\xi) = \mathbf{G}(x)\mathbf{K} + \mathbf{H}(x), \tag{39}$$

where **K** is the vector of constants, x^* is the lower integration bound for the different regions of the problem in Fig. 2. The parameters of the state vector can be expressed through:

$$Z_i^{(d)} = \sum_{j=1}^{r} G_{ij}^{(d)} K_j^{(d)} + H_j^{(d)}, Z_i^{(ud)} = \sum_{j=1}^{s} G_{ij}^{(ud)} K_j^{(ud)} + H_j^{(ud)}, \tag{40}$$

where subscript (*d*) = 1, 1a or 1q refers to the delaminated, while (*ud*) = 2 refers the undelaminated plate portion, *r* and *s* are the size of vectors and matrices of these parts, respectively.

A. Generalized Continuity Conditions

The generalized continuity conditions between regions 1 and 2 in Fig. 2 can be written as:

$$\begin{pmatrix} g_\alpha \\ h_\alpha \\ m_\alpha \\ n_\alpha \\ p_\alpha \end{pmatrix}|_{x=+0}^{(1)} = \begin{pmatrix} g_\alpha \\ h_\alpha \\ m_\alpha \\ n_\alpha \\ p_\alpha \end{pmatrix}|_{x=-0}^{(2)}, \tag{41}$$

where *g*, *h*, *m*, *n* and *p* denote parameter sets or functions defined in the sequel.

- *The continuity of deflection, its derivatives and the primary parameters* can be defined by a parameter set:

$$g_\alpha^{(l)} = (w, \frac{\partial w}{\partial x}, \ldots\ldots, \psi_{(p)j}; j = 1..\mathrm{Min}(q_l)), \tag{42}$$

where *l* is the actual region (1 or 2) and q_l is the number of parameters in $\psi_{(p)j}$ in both regions. We note that q_l is the total number of parameters in $\psi_{(p)j}$. As an example, for the TST model in Table I there are five parameters, on the other hand in Table II we have six, and thus for the TST theory with 4ESLs $\mathrm{Min}(q_l) = 5$.

- The continuity condition of membrane displacement parameters can be imposed by using the following functions [28]:

$$h_\alpha^{(1)} = \binom{u_{0b}}{v_{0b}} + \sum_{j=1}^{q_1} K_{1j}^{(0)} \binom{\psi_{(1)j}}{\psi_{(2)j}}|^{(1)},$$
$$h_\alpha^{(2)} = \binom{u_0}{v_0} + \sum_{j=1}^{q_2} K_{1j}^{(0)} \binom{\psi_{(1)j}}{\psi_{(2)j}}|^{(2)},$$
$$m_\alpha^{(1)} = \binom{u_{0t}}{v_{0t}} + \sum_{j=1}^{q_1} K_{3j}^{(0)} \binom{\psi_{(1)j}}{\psi_{(2)j}}|^{(1)},$$
$$m_\alpha^{(2)} = \binom{u_0}{v_0} + \sum_{j=1}^{q_2} K_{3j}^{(0)} \binom{\psi_{(1)j}}{\psi_{(2)j}}|^{(2)}. \tag{43}$$

In accordance with (41) the membrane displacement continuity requires the imposition of the conditions above for a single layer in the bottom and a single one in the top shell.

- Since q_l is not always the same number for the delaminated and undelaminated parts of the shell, it is required to define the so-called autocontinuity condition by:

$$n_\alpha^{(l)} = \sum_{j=1}^{q_l} K_{\kappa j}^{(\vartheta)} \binom{\psi_{(1)j}}{\psi_{(2)j}}|^{(l)}, \tag{44}$$

where ϑ = 1, 2, 3 depending on the vector of primary parameters (see Tables I and II).

- *The continuity conditions of stress resultants* can be defined by:

$$p_\alpha^{(l)} = (\sum_{i=1..k} \mathbf{N}_i^{(1,12)}, \hat{\mathbf{M}}_1^{(1,12)} \ldots, \hat{\mathbf{L}}_1^{(1,12)} \ldots, \hat{\mathbf{P}}_1^{(1,12)}, \ldots)|^{(l)}, \tag{45}$$

where the vectors including the hat mean equivalent stress resultants.

The continuity conditions between regions 1 - 1q and 1q - 1a for the problem in Fig. 2 are imposed by:

$$g_\beta^{(1)}|_{x=x_Q-d_0} = g_\beta^{(1q)}|_{x=x_Q-d_0},$$
$$g_\gamma^{(1)}|_{x=x_Q-d_0} = g_\gamma^{(1q)}|_{x=x_Q-d_0},$$
$$g_\beta^{(1q)}|_{x=x_Q+d_0} = g_\beta^{(1a)}|_{x=x_Q+d_0},$$
$$g_\gamma^{(1q)}|_{x=x_Q+d_0} = g_\gamma^{(1a)}|_{x=x_Q+d_0}, \tag{46}$$

where the parameter sets are [28]:

$$g_\beta^{(l)} = \left(w, \frac{\partial w}{\partial x}, \ldots\ldots, u_{0b}, u_{0t}, v_{0b}, v_{0t}, \psi_{(p)j}; j = 1..q_l\right), \quad p = 1,2,$$

$$g_\gamma^{(l)} = (\sum_{i=1}^{2} \mathbf{N}_i^{(1,12)}, \sum_{i=3}^{4} \mathbf{N}_i^{(1,12)}, \mathbf{M}_i^{(1,12)}.., \mathbf{L}_i^{(1,12)}.., \mathbf{P}_i^{(1,12)}..)|^{(l)} \tag{47}$$

where *i* = 1..4. It is important to note that (45) and (47) depend on the applied theory. As a matter of fact, for the FST model the conditions against **N** and **M** should be imposed, for the SST even the condition with respect to **L** is required, etc.

B. Boundary Conditions

The boundary conditions of the problem in Fig. 2 for the TST model are detailed here. The boundary conditions are imposed at region 1a in Fig. 2 as:

$$(w, v_{0b}, v_{0t}, \theta_{(\xi_2)1}, \theta_{(\xi_2)2}, \theta_{(\xi_2)3}, \theta_{(\xi_2)4}, \lambda_{(\xi_2)1}, \lambda_{(\xi_2)3})|_{x=a}^{(1a)} = 0,$$
$$(\sum_{i=1}^{2} N_{1(i)}, \sum_{i=3}^{4} N_{1(i)})|_{x=a}^{(1a)} = 0,$$

$$(M_{1(1)}, M_{1(2)}, M_{1(3)}, M_{1(4)}, P_{1(1)}, P_{1(3)})|_{x=a}^{(1a)} = 0. \quad (48)$$

For region 2 the conditions are:

$$(w, v_0, \theta_{(\xi_2)1}, \theta_{(\xi_2)2}, \theta_{(\xi_2)3}, \theta_{(\xi_2)4}, \lambda_{(\xi_2)3})|_{x=-c}^{(2)} = 0,$$
$$(\sum_{i=1}^{4} N_{1(i)}, M_{1(1)}, M_{1(2)}, M_{1(3)}, M_{1(4)}, P_{1(3)})|_{x=-c}^{(2)} = 0. \quad (49)$$

For the SST and FST theories the boundary conditions can be obtained similarly (refer to [28]).

TABLE III
ELASTIC PROPERTIES OF SINGLE CARBON/EPOXY COMPOSITE LAMINATES

	E_1 [GPa]	E_2 [GPa]	E_3 [GPa]
$\pm 45^f$	16.39	16.39	16.4
0	148	9.65	9.65
	G_{23} [GPa]	G_{13} [GPa]	G_{12} [GPa]
$\pm 45^f$	5.46	5.46	16.4
0	4.91	4.66	3.71
	ν_{23} [-]	ν_{13} [-]	ν_{12} [-]
$\pm 45^f$	0.5	0.5	0.3
0	0.27	0.25	0.3

In the next subsections the solution of the problem in Fig. 2 is presented. The lay-up of the shell is given by Fig. 1; the properties of layers are listed in Table III. The finite element model of the delaminated shell was also created in ANSYS environment, using 3D SOLID type elements. The mechanical fields were determined to verify the continuum model. In the vicinity of the delamination tip mesh refinement was done, please refer to [28] for more details. The geometrical data are: a = 105 mm, b = 100 mm, c = 45 mm and x_Q = 31 mm. The load is F = 1000 N. The lay-up of the plate is $[\pm 45^f/0/\pm 45^f_2/\underline{0}]_S$, which is shown in Fig. 1.

VI. RESULTS, DISPLACEMENT AND STRESS

Fig. 3 shows the deflection of the delaminated shell along the $y = b/2$ mid-line of the middle surface. The curves are determined by FST, SST, TST and FE analysis. It can be seen that the analytical model approximates very well the FE solution. A magnified view in the side of Fig. 3 indicates that the TST provides the highest deflection values and the FST results in the lowest ones.

The in-surface displacements along the cross section line of the delamination tip are evaluated in Fig. 4. The agreement among the analytical models and the FE solution is very good, however, it has to be mentioned that in the y direction the membrane displacement is smaller than that of the FE solution. On the other hand, the in-surface displacements are relatively small.

The normal stresses, σ_1 and σ_2 are evaluated in Fig. 5. The agreement is very good. The transverse shear stresses are plotted along the material lines in the middle ($y = b/2$) and in the edge ($y = 0$) of the shell in Fig. 6. It is shown that the FST provides the highest $\tau_{1\zeta}$ and $\tau_{2\zeta}$ shear stresses. The FE solution indicates a peak in the plane of delamination; this can be justified by the singular nature of FE solution, whereas the analytical solution is nonsingular. The $\tau_{2\zeta}$ transverse shear stress is plotted in Fig. 6 (b).

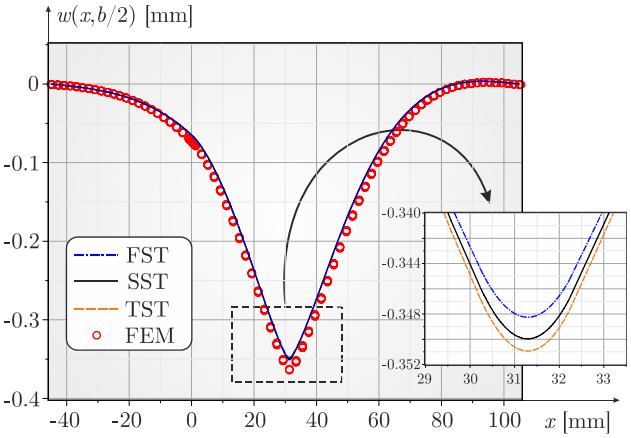

Fig. 3 Comparison of the deflection at y = b/2 calculated by FEM, FST, SST and TST using 4ESLs

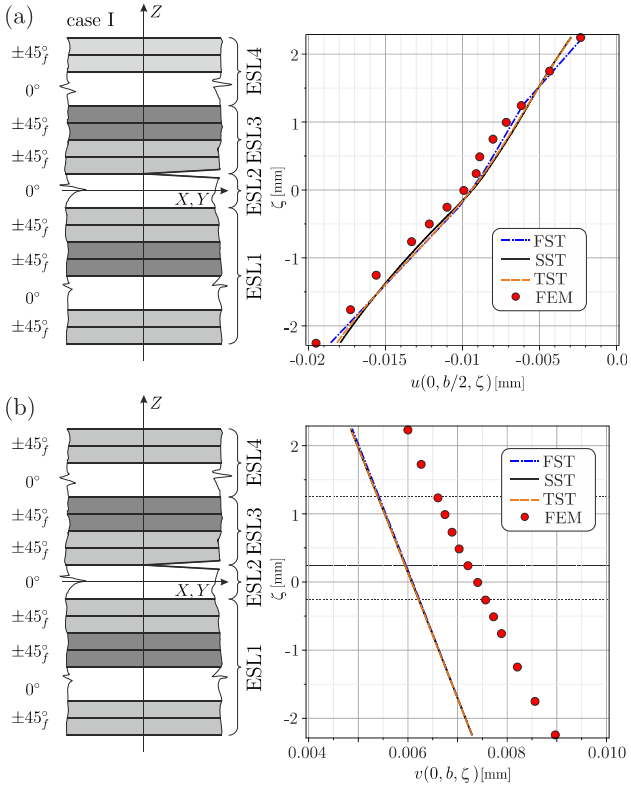

Fig. 4 Distribution of the in-plane displacements over the cross section of delamination tip by FEM, FST, SST and TST using 4ESLs

The agreement between the numerical and analytical solutions is poor, which can be justified by the fact that the evaluation was done at the edge of shell.

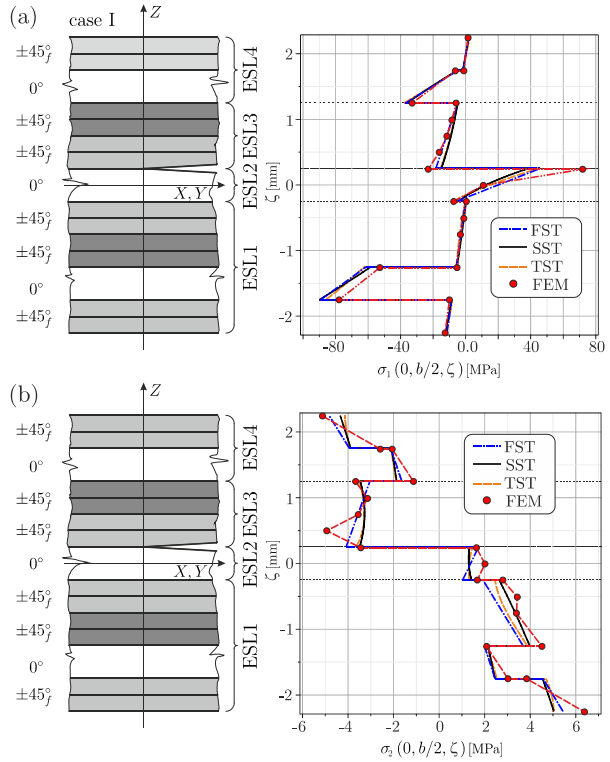

Fig. 5 Distribution of the normal stresses over the cross section of delamination tip by FEM, FST, SST and TST using 4ESLs

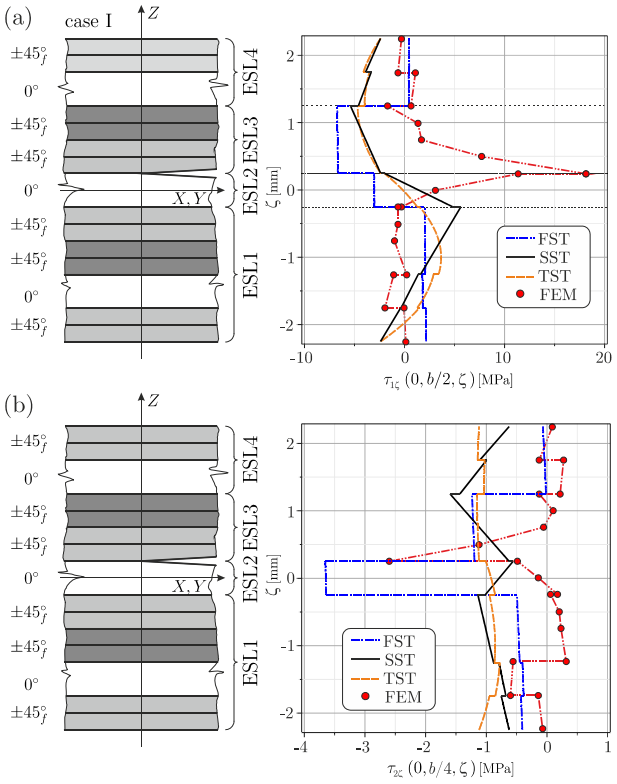

Fig. 6 Distribution of the transverse shear stresses over the cross section of delamination tip by FEM, FST, SST and TST using 4ESLs

The somewhat diverse results by analysis and FEM can be attributed to the different considerations of the two approximations. The analytical model is based on the assumptions of thin-walled structures. The delamination tip is not a singular point and the traction-free (or dynamic boundary) condition is not satisfied by any of the models. In contrast, the FE model does satisfy approximately the traction-free conditions at the boundary surfaces, moreover, the delamination tip is a singular type point, respectively. Because of the former reasons, a complete agreement between the analysis and FEM cannot be expected from the standpoint of displacement and stress. However, the deflection is a good and primary indicator to assess the accuracy of a continuum shell model. The secondary indicator is the energy release rate, which is determined by the J-integral.

VII. The J-integral

The general definition of the 3D J-integral is [22], [23]:

$$J_m = \int_C (\mathcal{W} n_m - \sigma_{ij} u_{i,m} n_j)\, ds + \int_A (\mathcal{W}\delta_{m3} - \sigma_{i3} u_{i,m})_{,3}\, dA, m = 1,2,3, \quad (50)$$

where C is a closed contour containing the delamination tip, W is the strain energy density, n m is the outward normal vector, σ_{ij} is the stress tensor, u_i is the displacement vector, s is the arc length coordinate along contour C, δ_{ij} is the Kronecker symbol and A is the area enclosed by contour C. Taking the special case discussed in this work ($J_1 = J_{II} + J_{III}$) and substituting back the stresses and strains by (17), (18) into (50) provides the mode-II and mode-III J-integrals. The mode-II J-integral becomes:

$$\begin{aligned} J_{II} = \tfrac{1}{2}\sum_{i=1}^{k}\{ & (N_{1(i)}\varepsilon^{(0)}_{1(i)}|^{(1)}_{x=+0} - N_{1(i)}\varepsilon^{(0)}_{1(i)}|^{(2)}_{x=-0}) - \\ & (N_{2(i)}\varepsilon^{(0)}_{2(i)}|^{(1)}_{x=+0} - N_{2(i)}\varepsilon^{(0)}_{2(i)}|^{(2)}_{x=-0}) + (M_{1(i)}\varepsilon^{(1)}_{1(i)}|^{(1)}_{x=+0} - \\ & M_{1(i)}\varepsilon^{(1)}_{1(i)}|^{(2)}_{x=-0}) - (M_{2(i)}\varepsilon^{(1)}_{2(i)}|^{(1)}_{x=+0} - M_{2(i)}\varepsilon^{(2)}_{2(i)}|^{(2)}_{x=-0}) + \\ & (L_{1(i)}\varepsilon^{(2)}_{1(i)}|^{(1)}_{x=+0} - L_{1(i)}\varepsilon^{(2)}_{1(i)}|^{(2)}_{x=-0}) - (L_{2(i)}\varepsilon^{(2)}_{2(i)}|^{(1)}_{x=+0} - \\ & L_{2(i)}\varepsilon^{(2)}_{2(i)}|^{(2)}_{x=-0}) + (P_{1(i)}\varepsilon^{(3)}_{1(i)}|^{(1)}_{x=+0} - P_{1(i)}\varepsilon^{(3)}_{1(i)}|^{(2)}_{x=-0}) - \\ & (P_{2(i)}\varepsilon^{(3)}_{2(i)}|^{(1)}_{x=+0} - P_{2(i)}\varepsilon^{(3)}_{2(i)}|^{(2)}_{x=-0})\}, \end{aligned} \quad (51)$$

where $k = 4$ because the method of 4ESLs is applied. The stress resultants are determined by (33), (34). The mode-III J-integral is:

$$\begin{aligned} J_{III} = -\tfrac{1}{2}\sum_{i=1}^{k}\{ & (N_{12(i)}\hat{\gamma}^{(0)}_{12(i)}|^{(1)}_{x=+0} - N_{12(i)}\hat{\gamma}^{(0)}_{12(i)}|^{(2)}_{x=-0}) + \\ & (M_{12(i)}\hat{\gamma}^{(1)}_{12(i)}|^{(1)}_{x=+0} - M_{12(i)}\hat{\gamma}^{(1)}_{12(i)}|^{(2)}_{x=-0}) + \\ & (L_{12(i)}\hat{\gamma}^{(2)}_{12(i)}|^{(1)}_{x=+0} - L_{12(i)}\hat{\gamma}^{(2)}_{12(i)}|^{(2)}_{x=-0}) + \\ & (P_{12(i)}\hat{\gamma}^{(3)}_{12(i)}|^{(1)}_{x=+0} - P_{12(i)}\hat{\gamma}^{(3)}_{12(i)}|^{(2)}_{x=-0})\}, \end{aligned} \quad (52)$$

where $k = 4$ and:

$$\hat{\gamma}^{(q)}_{12(i)} = \frac{\partial u^{(q)}_{(i)}}{\partial y} - \frac{\partial v^{(q)}_{(i)}}{\partial x}, q = 0,1,2,3, \quad (53)$$

are the so-called conjugate shear strains. Equations (51)-(53) are valid up to third-order shells and plates, however, it is easy to generalize for n^{th} order shells and plates as well. It is important to note that (51), (52) agree with the concept of [23]. As it can be seen, the mode-II J-integral is contributed by N_1, N_2, M_1, M_2, L_1, L_2, P_1 and P_2, on the other hand the mode-III J-integral contains N_{12}, M_{12}, L_{12} and P_{12}. In the sequel the results of the method of 4ESLs (FST, SST, TST) are presented and compared to the results of FE analysis obtained by using the virtual crack closure technique (VCCT).

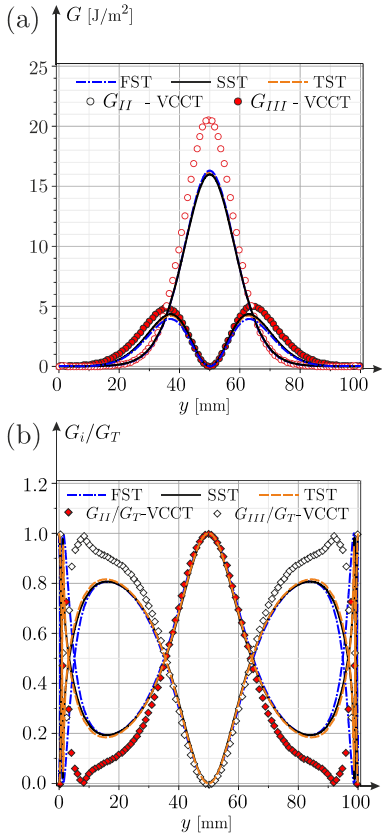

Fig. 7 Distribution of the ERRs and mode mixity along the delamination front by FEM, FST, SST and TST using 4ESLs. $G_T = G_{II} + G_{III}$ is the total energy release rate

Under static conditions the J-integral is equivalent to the energy release rate, i.e.: $J_{II} \equiv G_{II}$ and $J_{III} \equiv G_{III}$. The distribution of mode-II and mode-III ERRs is depicted Fig. 7 (a). The FE solution was obtained by the VCCT. The analytical shell models provide a very good fit of the numerical solution, however, the mode-II ERR is a little bit higher from the FE model. The mode ratios are plotted in Fig. 7 (b). Again, the agreement is quite good in the middle region of the delamination front, around the edges the analytical models do not agree with the numerical points. The final conclusion is that in fact the FST shell theory is capable to describe as accurately the mechanical fields and the energy release rates as the SST and TST. However, because of the continuity conditions the latter theories result in smaller model size than the FST.

VIII. Conclusions

In this work, a delaminated shell was modeled by higher-order shell theories through a semi-layerwise modelling technique applying four ESL along the thickness of shell. In the first step, the assumed displacement field was created using third-order Taylor expansion. By means of the displacement field, the strain field was generated by the equations of shell theory. The stress field was determined based on the constitutive equation of orthotropic solids under plane stress assumption. Then, the virtual work principle was applied to obtain the invariant form of governing system of PDE for the undelaminated and delaminated parts of the shell system. The equations of third-, second- and first-order shells were equally derived.

The system of equations was solved by the Lévy method applying simply supported edges. Thus, a system of ordinary differential equations was obtained, which was solved by the state space approach. The continuity conditions between the delaminated and undelaminated parts were given, as well as the boundary conditions. The obtained boundary value problem solution was utilized to determine the mechanical (displacement, strain and stress) fields and the J-integral. The 3D numerical (finite element) model of the delaminated composite shell was also created for comparison purposes with the analytical approach. The performed work and results led to the following conclusions: The mechanical fields in cross sections along the delamination front are strongly perturbated. The analytical and finite element models are based on different considerations and so the usual agreement between the two methods, which exists in shells without material defects, is not obtained in this work. However, the transverse deflection was found to be a primary indicator to assess the suitability of a continuum shell model in light of the finite element solution. The secondary indicator was the distribution of energy release rates and mode ratios along the delamination front. In this respect the shell model agreed very well with the results of numerical model. It was also concluded that the first-order model provides as good approximation as the second- or third-order models; however, the latter involves smaller model size. Continuing the work, other shell theories are desired to try out for the same problem. Besides, it is also required to implement the J-integral into the 3D finite element model, since ANSYS is not able to determine J for orthotropic materials. For this reason, the energy release rates were determined by the virtual crack closure method, which - although widely accepted - is based on different considerations than the J-integral. These tasks are going to be achieved in the near future.

Acknowledgment

This work was supported by the Hungarian Scientific Research Fund (NKFI) under grant No.128090. The research reported in this paper was supported by the Higher Education Excellence Program of the Ministry of Human Capacities in

the frame of TOPIC research area of Budapest University of Technology and Economics (BME FIKP-NANO).

REFERENCES

[1] L. N. Phillips, Ed., *Design with Advanced Composite Materials*. Berlin, Heidelberg, New York, London, Paris, Tokyo: Springer-Verlag, The Design Council, 1989.
[2] J. N. Reddy, *Mechanics of laminated composite plates and shells - Theory and analysis*. Boca Raton, London, New York, Washington D.C.: CRC Press, 2004.
[3] D. F. Adams, L. A. Carlsson, and R. B. Pipes, *Experimental characterization of advanced composite materials*, Third ed. Boca Raton, London, New York, Washington, D.C.: CRC Press, 2000.
[4] T. L. Anderson, *Fracture Mechanics - Fundamentals and Applications*, Third ed. Boca Raton, London, New York, Singapore: CRC Press, Taylor & Francis Group, 2005.
[5] J. Jumel, M. K. Budzik, and M. E. R. Shanahan, "Beam on elastic foundation with anticlastic curvature: Application to analysis of mode I fracture tests," *Engineering Fracture Mechanics*, vol. 78, no. 18, pp. 3253–3269, 2011.
[6] J. Jumel, M. K. Budzik, and M. E. R. Shanahan, "Process zone in the single cantilever beam under transverse loading. part I: Theoretical analysis," *Theoretical and Applied Fracture Mechanics*, vol. 56, no. 1, pp. 7–12, 2011.
[7] A. Szekrényes, "Improved analysis of unidirectional composite delamination specimens," *Mechanics of Materials*, vol. 39, pp. 953–974, 2007.
[8] M. G. Andrews and R. Massabò, "The effects of shear and near tip deformations on energy release rate and mode mixity of edge-cracked orthotropic layers," *Engineering Fracture Mechanics*, vol. 74, pp. 2700-2720, 2007.
[9] M. Pelassa and R. Massabò, "Explicit solutions for multi-layered wide plates and beams with perfect and imperfect bonding and delaminations under thermo-mechanical loading," *Meccanica*, vol. 50, no. 10, pp. 2497–2524, 2015.
[10] B. D. Davidson, L. Yu, and H. Hu, "Determination of energy release rate and mode mix in three-dimensional layered structures using plate theory," *International Journal of Fracture*, vol. 105, pp. 81–104, 2000.
[11] B. V. Sankar and V. Sonik, "Pointwise energy release rate in delaminated plates," *AIAA Journal*, vol. 33, no. 7, pp. 1312–1318, 1995.
[12] C. K. Hirwani, S. K. Panda, and T. R. Mahapatra, "Nonlinear finite element analysis of transient behavior of delaminated composite plate," *Journal of Vibration and Acoustics*, vol. 140, no. 2, p. 021001, 2018.
[13] A. Szekrényes, "Bending solution of third-order orthotropic Reddy plates with asymmetric interfacial crack," *International Journal of Solids and Structures*, vol. 51, pp. 2598–2619, 2014.
[14] N. Nanda and S. Sahu, "Free vibration analysis of delaminated composite shells using different shell theories," *International Journal of Pressure Vessels and Piping*, vol. 98, pp. 111 – 118, 2012.
[15] S. K. Panda and B. N. Singh, "Large amplitude free vibration analysis of thermally post-buckled composite doubly curved panel using nonlinear FEM," *Finite Elements in Analysis and Design*, vol. 47, pp. 378–386, 2011.
[16] V. K. Singh and S. K. Panda, "Nonlinear free vibration analysis of single/doubly curved composite shallow shell panels," *Thin-Walled Structures*, vol. 85, pp. 431–349, 2014.
[17] L. P. Kollár and G. S. Springer, *Mechanics of Composite Structures*. Cambridge, New York, Melbourne, Madrid, Cape Town, Singapore, Sao Paolo: Cambridge University Press, 2003.
[18] A. Szekrényes, "Nonsingular crack modelling in orthotropic plates by four equivalent single layers," *European Journal of Mechanics A/Solids*, vol. 55, pp. 73–99, 2016.
[19] A. Szekrényes, "Semi-layerwise analysis of laminated plates with nonsingular delamination - the theorem of autocontinuity," *Applied Mathematical Modelling*, vol. 40, pp. 1344–1371, 2016.
[20] N. Nanda, "Static analysis of delaminated composite shell panels using layerwise theory," *Acta Mechanica*, vol. 225, no. 10, pp. 2893–2901, 2014.
[21] A. Szekrényes, "The role of transverse stretching in the delamination fracture of softcore sandwich plates," *Applied Mathematical Modelling*, vol. 63, pp. 611–632, 2018.
[22] K. N. Shivakumar and I. S. Raju, "An equivalent domain integral method for three-dimensional mixed-mode fracture problems," *Engineering Fracture Mechanics*, vol. 42, no. 6, pp. 935–959, 1992.
[23] R. H. Rigby and M. H. Aliabadi, "Decomposition of the mixed-mode J-integral - revisited," *International Journal of Solids and Structures*, vol. 35, no. 17, pp. 2073–2099, 1998.
[24] J. Petrolito, "Vibration and stability analysis of thick orthotropic plates using hybrid-Trefftz elements," *Applied Mathematical Modelling*, vol. 38, no. 24, pp. 5858–5869, 2014.
[25] M. Izadi and M. Tahani, "Analysis of interlaminar stresses in general cross-ply laminates with distributed piezoelectric actuators," *Composite Structures*, no. 92, pp. 757–768, 2010.
[26] A. Szekrényes, "The system of exact kinematic conditions and application to delaminated first-order shear deformable composite plates," *International Journal of Mechanical Sciences*, vol. 77, pp. 17–29, 2013.
[27] A. Szekrényes, "Antiplane-inplane shear mode delamination between two second-order shear deformable composite plates," *Mathematics and Mechanics of Solids*, pp. 1–24, 2015.
[28] A. Szekrényes, *Nonsingular delamination modeling in orthotropic composite plates by semi-layerwise analysis*. Hungarian Academy of Sciences, D.Sc. dissertation, December 2017.
[29] Y. Jianqiao, *Laminated Composite Plates and Shells - 3D modelling*. London, Berlin, Heidelberg, New York, Hong Kong, Milan, Paris, Tokyo: Springer, 2003.

A. Szekrényes graduated from the Department of Applied Mechanics, Faculty of Mechanical Engineering, Budapest University of Technology and Economics (BME), Budapest, Hungary, in 2000. He continued his research in the field of fracture mechanics and mechanics of composite materials within the scope of a national doctoral program at BME and obtained his Ph.D. degree in 2006. In 2007 he became an Assistant Professor and in 2011 Associate Professor at the Department of Applied Mechanics. In 2016 he was awarded the Bolyai János plaquette by the Hungarian Academy of Sciences. In 2017 he defended his D.Sc. degree at the Hungarian Academy of Sciences in the field of mechanics. He published 49 papers in international journals and took part in several international conferences. Dr. Szekrényes is available as reviewer in several international journals.